

# Scalar revelations at future $e^+e^-$ colliders



Howard E. Haber  
13 September 2023



# References

1. ILC Higgs White Paper, arXiv:[1310.0763](https://arxiv.org/abs/1310.0763)
2. The International Linear Collider--A Global Project, arXiv:[1903.01629](https://arxiv.org/abs/1903.01629)
3. Physics Briefing Book (Input for the European Strategy for Particle Physics Update 2020), arXiv:[1910.11775](https://arxiv.org/abs/1910.11775)
4. The International Linear Collider—Report to Snowmass 2021, arXiv:[2203.07622](https://arxiv.org/abs/2203.07622)
5. Report of the Snowmass 2021  $e^+ e^-$  Collider Forum, arXiv:[2209.03472](https://arxiv.org/abs/2209.03472)
6. The Energy Frontier Report (2021 US Community Study on the Future of Particle Physics), arXiv:[2211.11084](https://arxiv.org/abs/2211.11084)
7. Report of the Topical Group on Higgs Physics for the Energy Frontier: The Case for Precision Higgs Physics, arXiv:[2211.11084](https://arxiv.org/abs/2211.11084)
8. Michael Peskin, Model-Agnostic Exploration of the Mass Reach of Precision Higgs Boson Coupling Measurements, arXiv:[2209.03303](https://arxiv.org/abs/2209.03303)

Thanks to Michael Peskin and Georg Weiglein for providing some additional material for this talk.

## Where do we stand today?

Eleven years since the discovery of the Higgs boson at the LHC, roughly 9 million Higgs bosons having been produced in Runs 1 and 2 (although only about 0.3% of these produced Higgs bosons can be detected by the ATLAS and CMS Collaborations).

Measurements of total and differential cross sections, branching fractions, and other properties of the Higgs boson have revealed the existence of a scalar particle that closely resembles the predicted Higgs boson of the Standard Model (SM). Nevertheless, the current accuracy of the Higgs data still leaves plenty of room for possible deviations from the SM.

# Summary of ATLAS Higgs boson data from Run 2 at the LHC

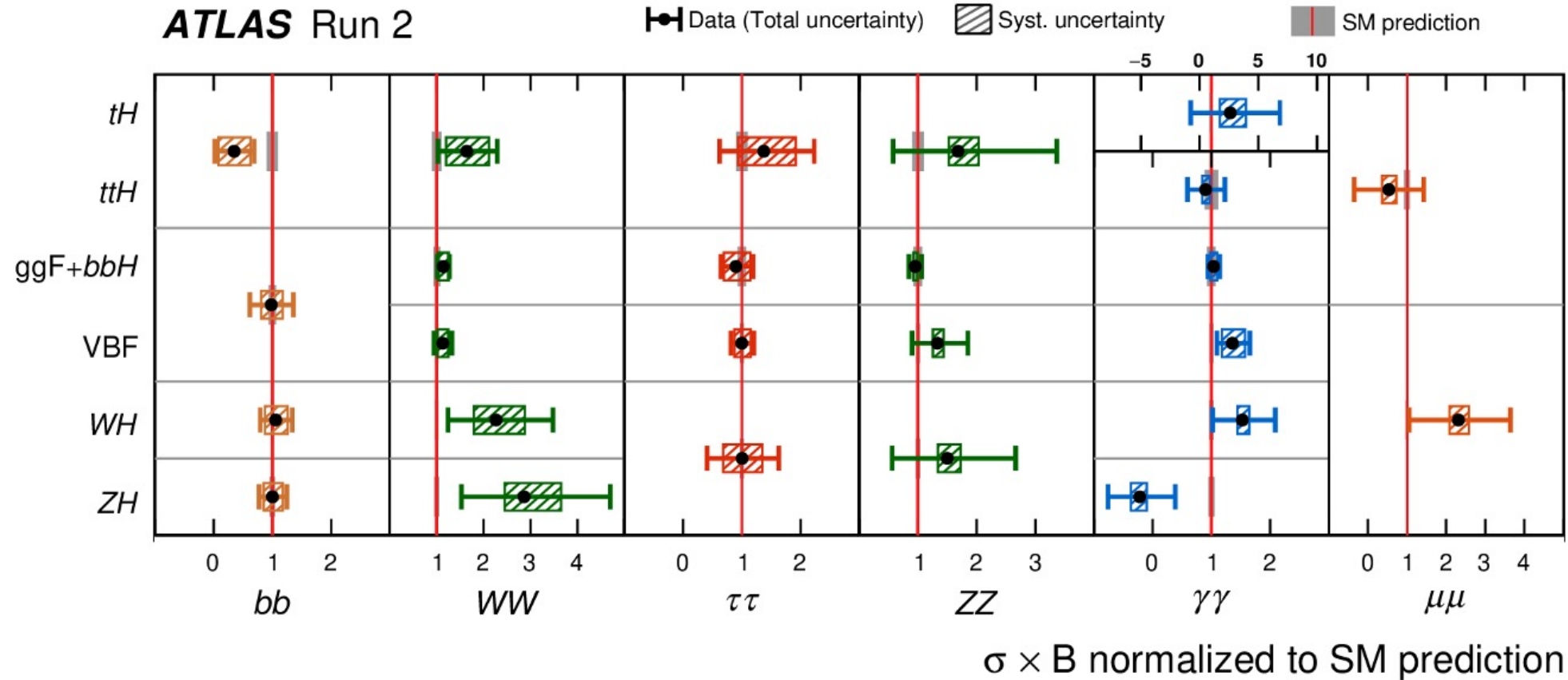
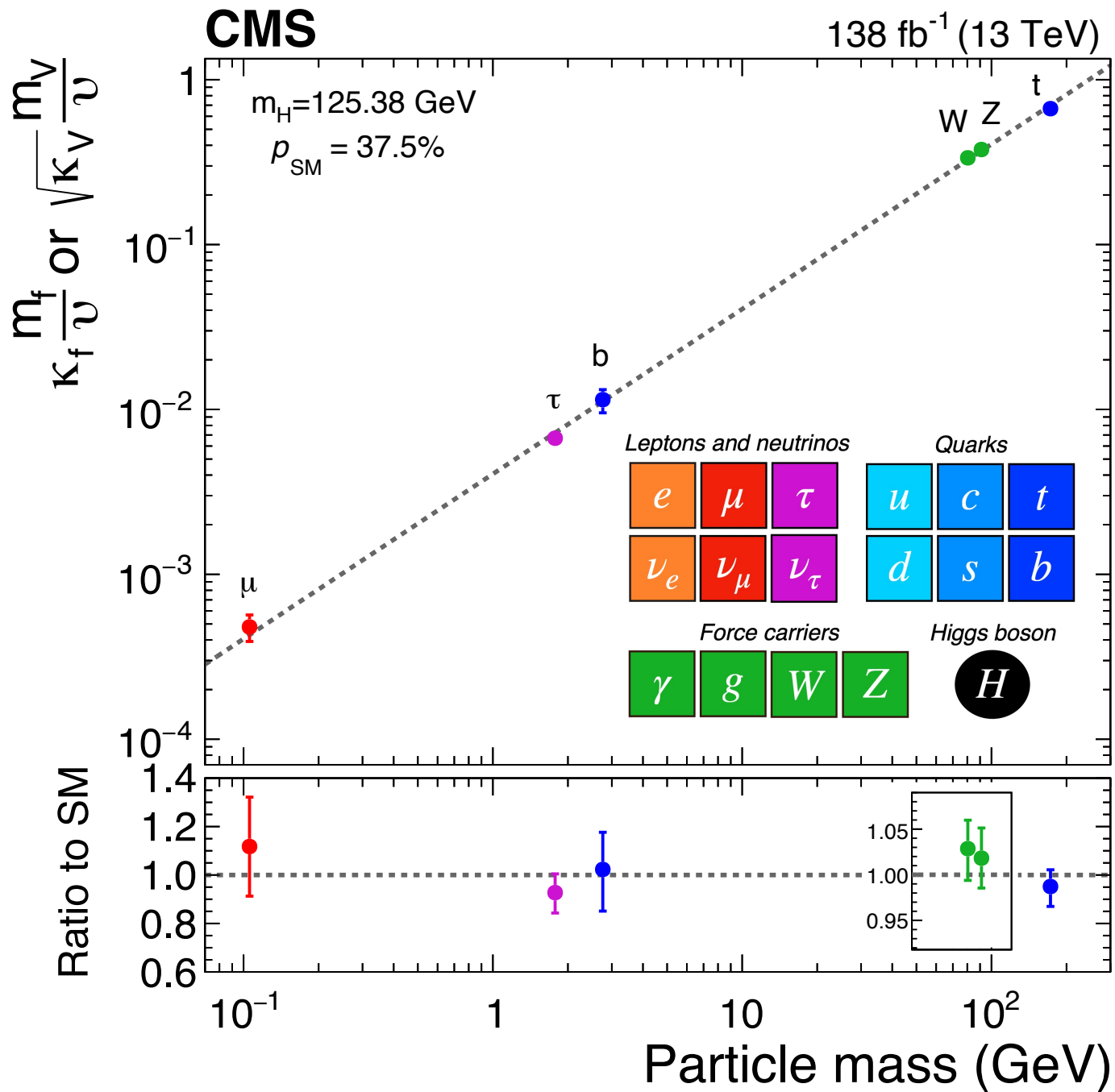


**Fig. 3 | Ratio of observed rate to predicted standard model event rate for different combinations of Higgs boson production and decay processes.** The horizontal bar on each point denotes the 68% confidence interval. The narrow grey bands indicate the theory uncertainties in the standard model

(SM) cross-section multiplied by the branching fraction predictions. The  $p$  value for compatibility of the measurement and the SM prediction is 72%.  $\sigma_i B_f$  is normalized to the SM prediction. Data are from ATLAS Run 2.



From the CMS  
 webpage

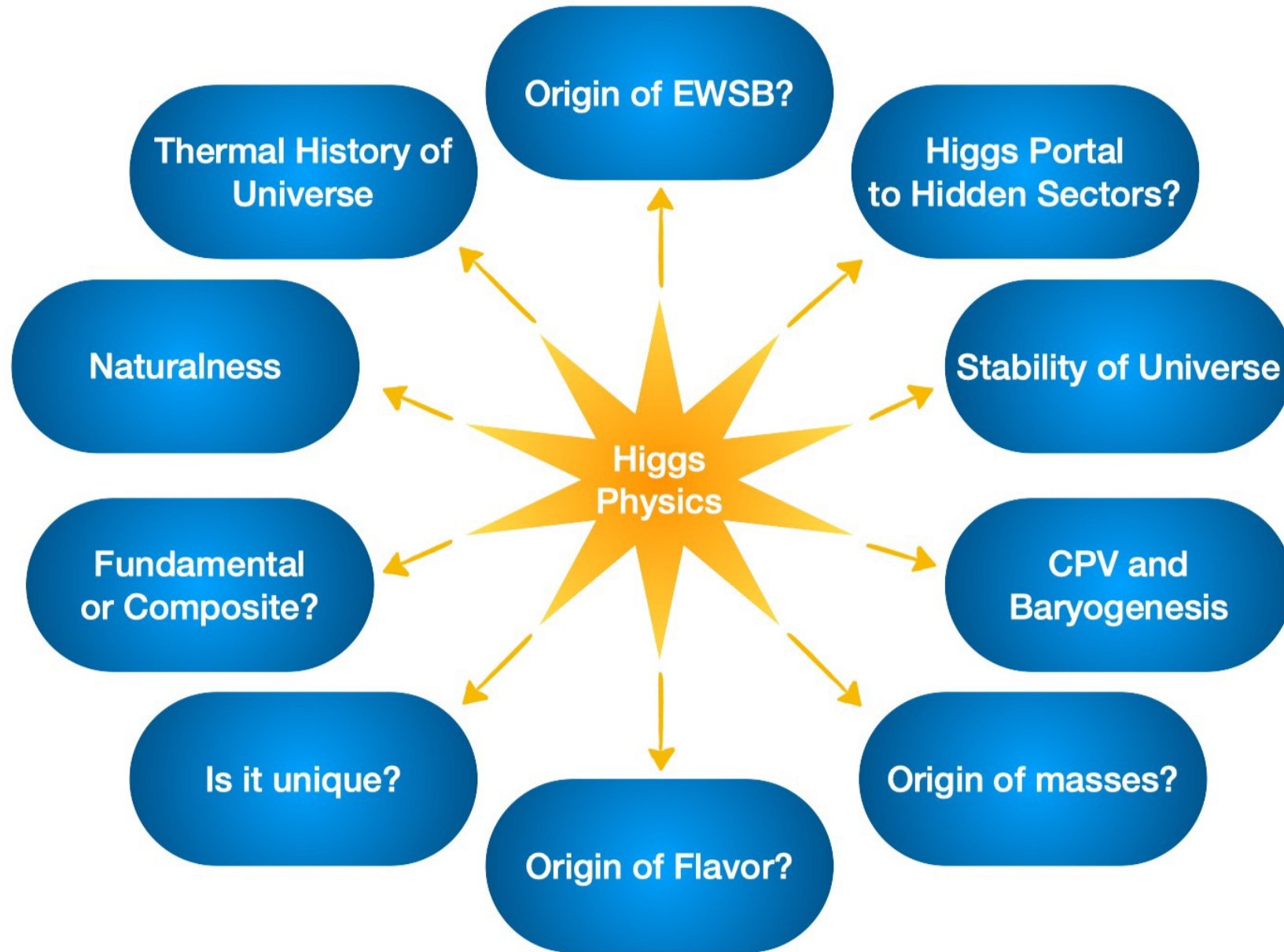
Reduced Higgs coupling modifiers compared to their corresponding prediction from the Standard Model (SM). The error bars represent 68% CL intervals for the measured parameters. In the lower panel, the ratios of the measured coupling modifiers values to their SM predictions are shown.

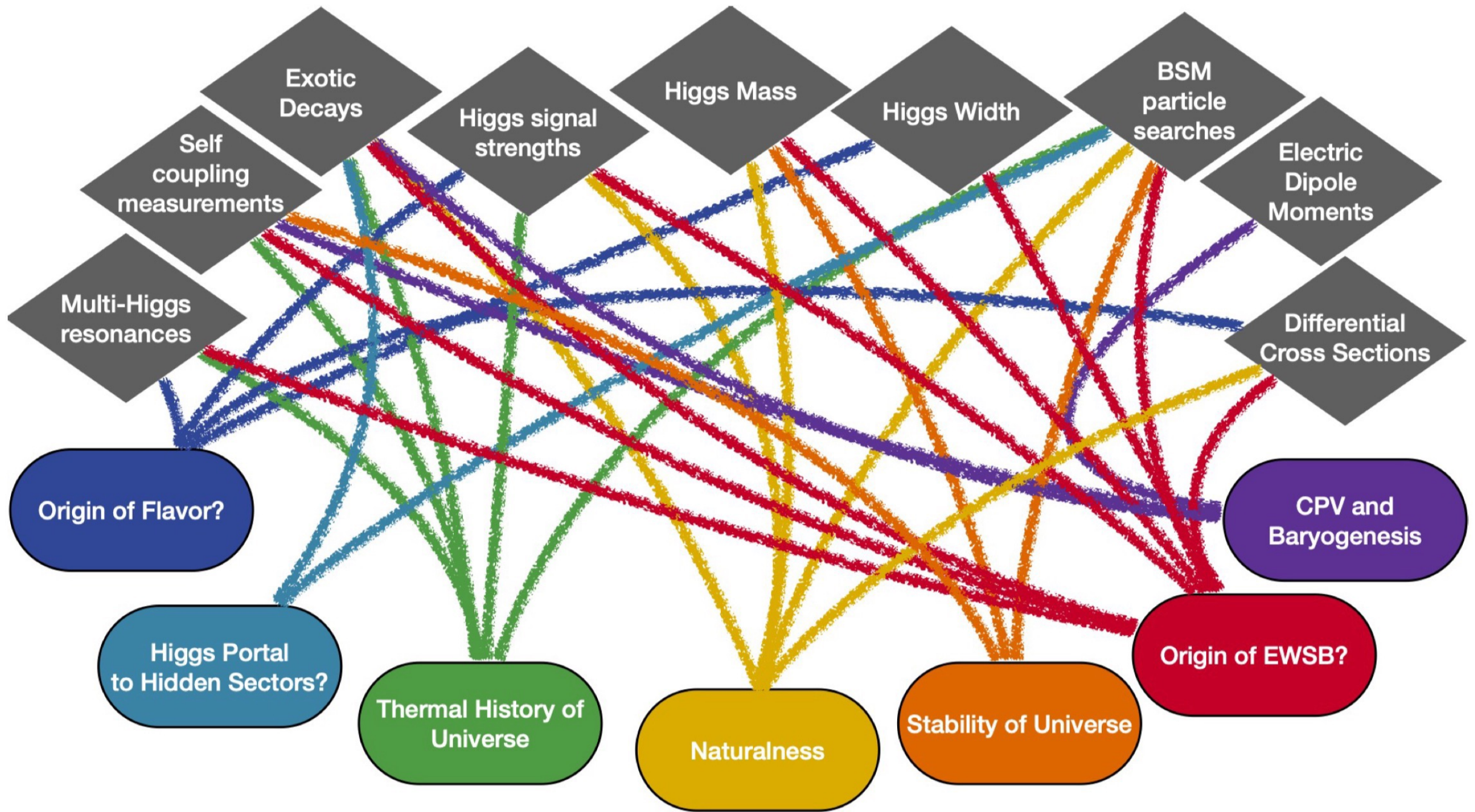
## Looking Forward...

Run 3 of the LHC (2022—2025) anticipates doubling the size of the Run 2 Higgs data set. The High Luminosity (HL) LHC ultimately expects a total integrated luminosity of about 20 times the size of the Run 2 Higgs data set.

Even with such an increase in the precision of Higgs measurements, some of the most pressing questions associated with the Higgs boson may lie beyond the LHC.

Future high energy  $e^+e^-$  colliders now under consideration can provide the critical next step in pursuing the fundamental questions associated with Higgs boson physics.







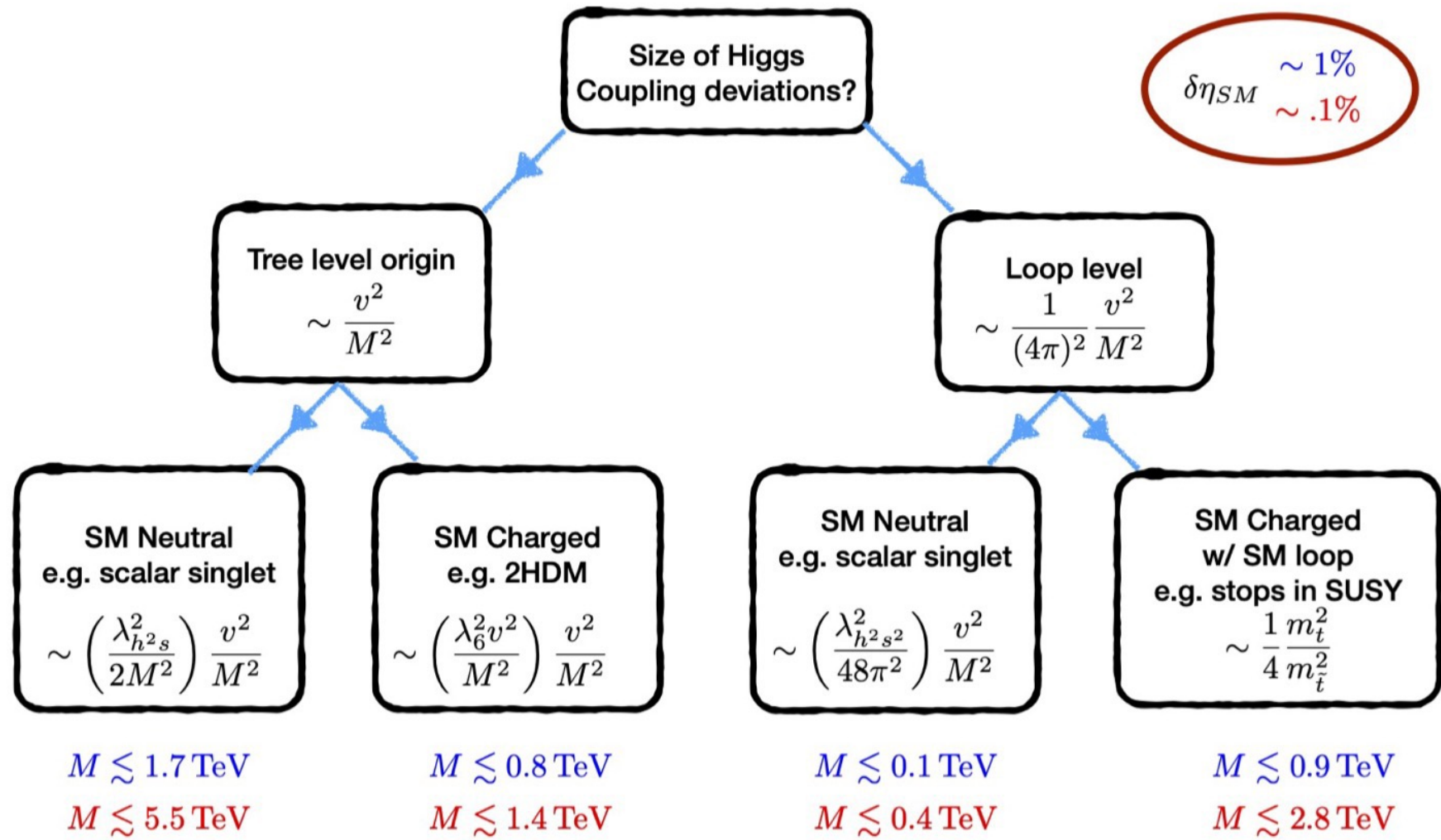
# Goals of future Higgs studies

The Higgs sector is likely to be involved with many of the unanswered questions of fundamental physics that cannot be addressed by the SM. These include CP violation and baryogenesis, the origin of flavor, neutrino masses, the origin of the electroweak symmetry breaking (EWSB) scale, early universe dynamics, etc.

Precision studies of the Higgs boson properties will play a critical role in revealing deviations from the Standard Model that can provide important clues for constructing a more fundamental theory of physics beyond the SM (BSM).

# How the effects of BSM physics are reflected in precision Higgs studies

1. Accessing a new (higher) mass scale via decoupling.
  - If  $v = 246$  GeV is the scale of EWSB and  $M$  is the mass scale of new BSM physics, then deviations from the SM (viewed as an effective low-energy theory) are typically suppressed by  $v^2/M^2$ .
2. Accessing a new (feeble) coupling via the Higgs portal.
  - If  $\phi$  is the doublet Higgs field of the SM, then  $\phi^\dagger\phi$  is a SM gauge group singlet that can couple to a “dark” sector. If  $D$  is a singlet field then a term  $\phi^\dagger\phi f(D)$  in the Lagrangian generates a mixing of the SM Higgs field  $\phi$  with new BSM fields thereby modifying the SM couplings of the Higgs boson. Note that  $D$  can be a composite field operator made up of fields with nonzero SM gauge charges.

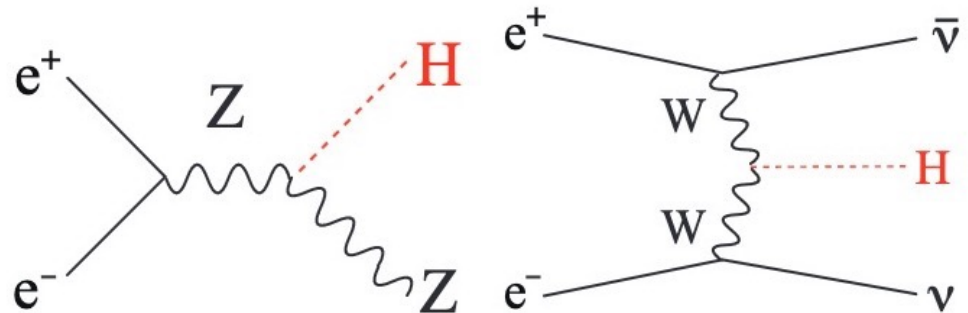


**Conservative Scaling for Upper Limit on Mass Scale Probed by Higgs Precision**

FIG. 3: Typical Higgs coupling deviations depending on whether the couplings are generated from new physics that generates tree level effects or loop level effects primarily. Optimistically assuming all new physics couplings or ratios of new physics scales are  $\mathcal{O}(1)$  gives a conservative upper bound on the highest scales probed by Higgs coupling deviations. Based on assuming a precision for Higgs coupling deviations of  $1 \rightarrow .1\%$  this shows that Higgs couplings probe scales from as weak as  $M \sim 100 \text{ GeV}$  to as strong as  $M \sim 5.5 \text{ TeV}$ .

# What is the target precision for future Higgs studies?

- The current LHC Higgs data has reached a level of roughly 10% precision in measurements of signal strengths. Note that if, e.g.,  $M = 2 \text{ TeV}$ , then  $v^2/M^2 \simeq 0.015$ . It is not surprising that current LHC measurements of Higgs couplings are not particularly sensitive to new TeV-scale physics.
- Deviations from SM behavior will only be convincing if the dominant uncertainties are statistical (which can be further improved with more data). Future  $e^+e^-$  colliders provide this opportunity due to their relatively clean environment and two dominant production mechanisms ( $e^+e^- \rightarrow Z h$  and  $W^*W^* \rightarrow h$ ).



## Example: The CP-conserving 2HDM

The two-Higgs doublet model (2HDM) consists of two  $Y = 1$  scalar doublet fields  $\Phi_1$  and  $\Phi_2$ . In the Higgs basis, one defines two new linear combinations  $\{\mathcal{H}_1, \mathcal{H}_2\}$  where  $\langle \mathcal{H}_1^0 \rangle = v/\sqrt{2}$  and  $\langle \mathcal{H}_2^0 \rangle = 0$ , with  $v \simeq 246$  GeV. If  $\varphi^0 \equiv \sqrt{2} \text{Re } \mathcal{H}_1^0 - v$  were a mass eigenstate, then its tree-level properties would coincide with those of the SM Higgs boson.

The scalar potential contains the term

$$\mathcal{V} \supset \frac{1}{2} Z_1 (\mathcal{H}_1^\dagger \mathcal{H}_1)^2 + \{ Z_6 (\mathcal{H}_1^\dagger \mathcal{H}_1) (\mathcal{H}_1^\dagger \mathcal{H}_2) + \text{h.c.} \},$$

which generates mixing between  $\varphi^0$  and  $\sqrt{2} \text{Re } \mathcal{H}_2^0$ .

Denoting the two CP-even neutral scalar mass eigenstates by  $h$  and  $H$  (with  $m_h < m_H$ )

$$\begin{pmatrix} H \\ h \end{pmatrix} = \begin{pmatrix} c_{\beta-\alpha} & -s_{\beta-\alpha} \\ s_{\beta-\alpha} & c_{\beta-\alpha} \end{pmatrix} \begin{pmatrix} \sqrt{2} \operatorname{Re} \mathcal{H}_1^0 - v \\ \sqrt{2} \operatorname{Re} \mathcal{H}_2^0 \end{pmatrix}.$$

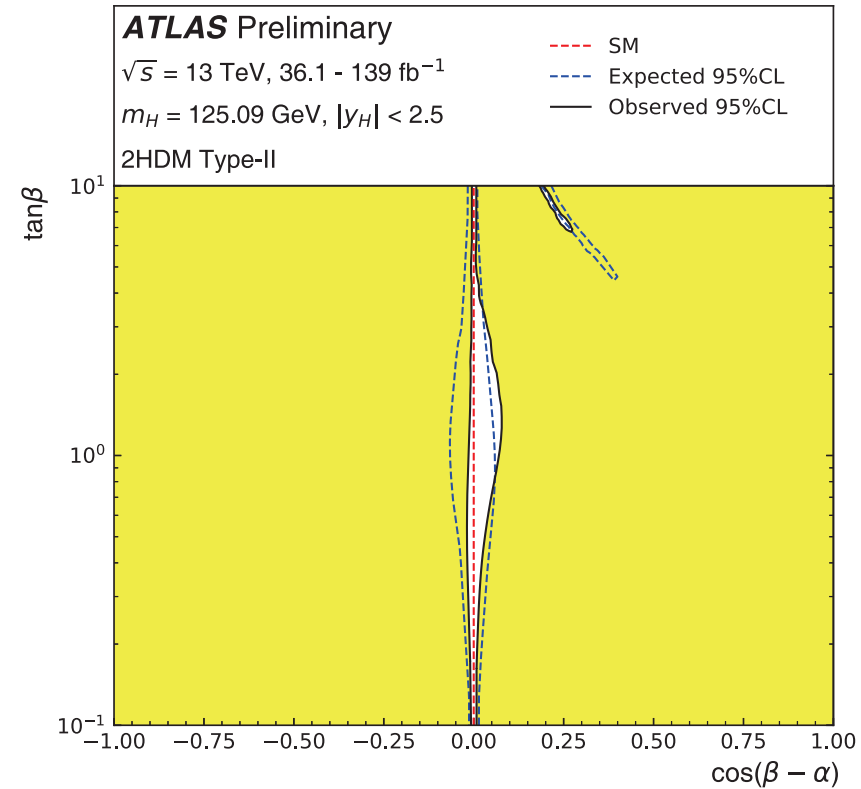
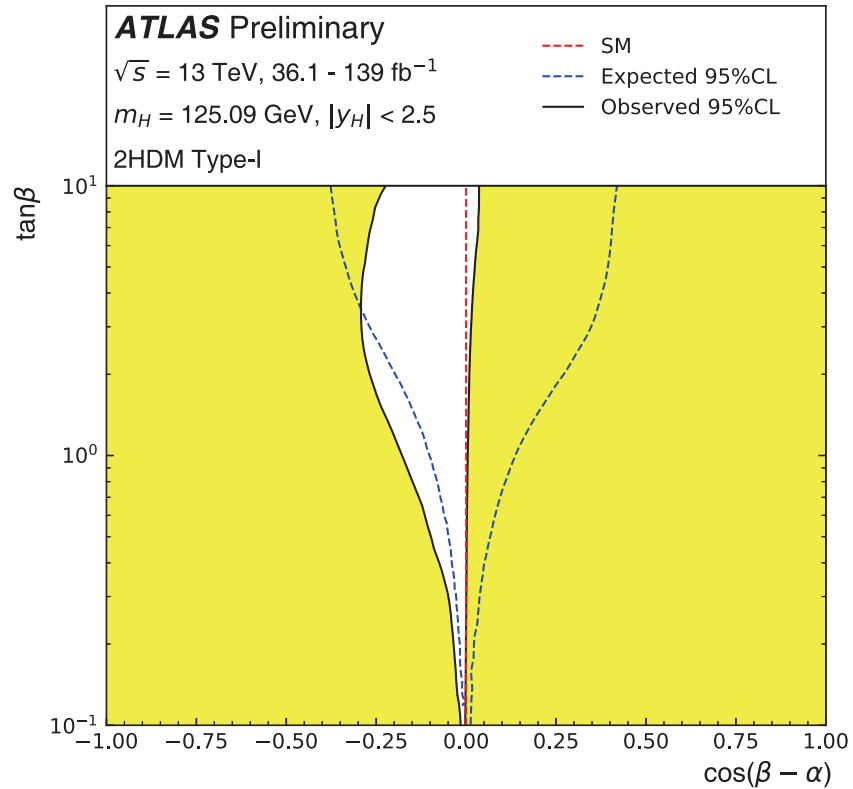
If  $h$  is SM-like, then  $m_h^2 \simeq Z_1 v^2$  (i.e.,  $Z_1 \simeq 0.26$ ) and

$$|c_{\beta-\alpha}| = \frac{|Z_6|v^2}{\sqrt{(m_H^2 - m_h^2)(m_H^2 - Z_1 v^2)}} \simeq \frac{|Z_6|v^2}{m_H^2 - m_h^2} \ll 1,$$

This is the so-called Higgs alignment limit, which is achieved if

1.  $m_H^2 \gg |Z_6|v^2$ , corresponding to the *decoupling limit*; and/or
2.  $|Z_6| \ll 1$ , corresponding to a feeble Higgs portal coupling.

# LHC constraints on Higgs alignment in the 2HDM



Regions excluded by fits to the measured rates of the productions and decay of the Higgs boson (assumed to be  $h$  of the 2HDM). Contours at 95% CL. The observed best-fit values for  $\cos(\beta - \alpha)$  are  $-0.006$  for the Type-I 2HDM and  $0.002$  for the Type-II 2HDM. Taken from ATLAS Collaboration, ATLAS-CONF-2021-053 (2 November 2021).

## Deviations of the couplings of $h$ from their SM values

$$\begin{aligned} \mathcal{L}_{\text{int}} \supset & \left( gm_W W_\mu^+ W^{\mu-} + \frac{g}{2c_W} m_Z Z_\mu Z^\mu \right) s_{\beta-\alpha} h \\ & - \bar{U} \left\{ \frac{\mathbf{M}_U}{v} s_{\beta-\alpha} + \frac{1}{\sqrt{2}} c_{\beta-\alpha} [\boldsymbol{\rho}^U P_R + (\boldsymbol{\rho}^U)^\top P_L] \right\} U h \\ & - \bar{D} \left\{ \frac{\mathbf{M}_D}{v} s_{\beta-\alpha} + \frac{1}{\sqrt{2}} c_{\beta-\alpha} [(\boldsymbol{\rho}^D)^\top P_R + \boldsymbol{\rho}^D P_L] \right\} D h, \end{aligned}$$

where  $P_{R,L} \equiv \frac{1}{2}(1 \pm \gamma_5)$  and the mass-eigenstate quark fields are  $D = (d, s, b)^\top$ ,  $U \equiv (u, c, t)^\top$ , with corresponding diagonal mass matrices  $\mathbf{M}_F$  and independent Yukawa matrices  $\boldsymbol{\rho}^F$  ( $F = U, D$ ). Note that for Type I Yukawa couplings,  $\boldsymbol{\rho}^F = \sqrt{2} \mathbf{M}_F \cot \beta / v$ . For Type II Yukawa couplings, replace  $\cot \beta$  with  $-\tan \beta$  in  $\boldsymbol{\rho}^D$ .



In the decoupling limit,  $c_{\beta-\alpha} \sim v^2/M^2$ , where  $M$  is the mass scale of the heavy scalars of the 2HDM. Thus,

$$g_{hVV} \sim \frac{v^4}{M^4}, \quad g_{hFF} \sim \frac{v^2}{M^2}.$$

The  $hFF$  couplings can be further enhanced in some cases. For example, in the Type II 2HDM,

$$g_{hUU} \sim \frac{v^2 \cot \beta}{M^2}, \quad g_{hDD} \sim \frac{v^2 \tan \beta}{M^2}.$$

# A Landscape of possible future $e^+e^-$ colliders

Collider	$\sqrt{s}$	P [%] $e^-/e^+$	$L_{\text{int}}$ $\text{ab}^{-1}$
ILC	250 GeV	$\pm 80 / \pm 30$	2
	350 GeV	$\pm 80 / \pm 30$	0.2
	500 GeV	$\pm 80 / \pm 30$	4
	1 TeV	$\pm 80 / \pm 20$	8
ILC-GigaZ	$m_Z$	$\pm 80 / \pm 30$	0.1
CLiC	380 GeV	$\pm 80 / 0$	1
	500 GeV	$\pm 80 / 0$	2.5
	1 TeV	$\pm 80 / 0$	5
CEPC	$m_Z$		60 / 100
	$2m_W$		3.6 / 6
	240 GeV		12 / 20
	$2m_t$		- / 1
FCC-ee	$m_Z$		150
	$2m_W$		10
	240 GeV		5
	$2m_t$		1.5

Table 2: Running scenarios used for the Snowmass 21 studies.

# Higgs boson production processes at the ILC

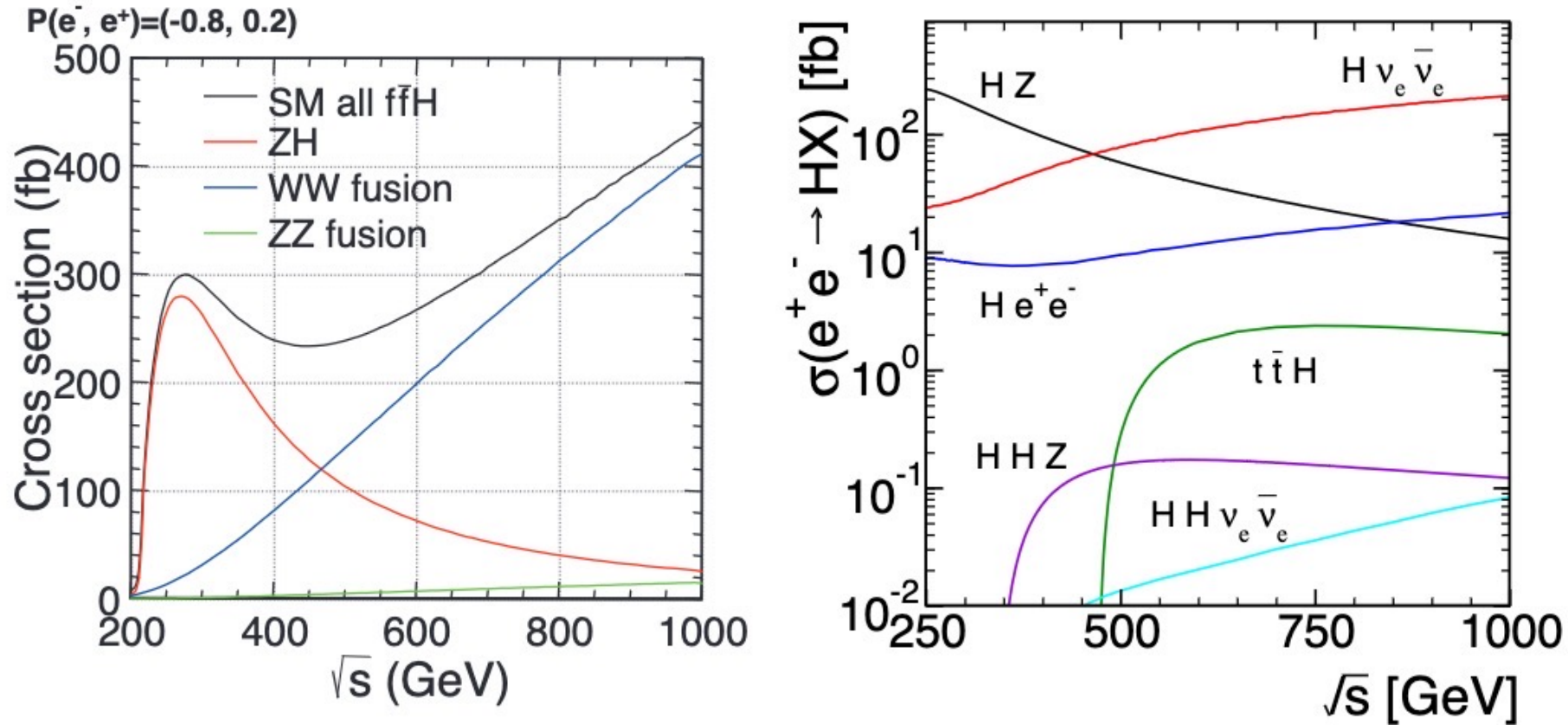


**Figure 1.4.** (Left) The production cross sections of the Higgs boson with the mass of 125 GeV at the ILC as a function of the collision energy  $\sqrt{s}$ . Polarization of the electron beam (80%) and the positron beam (20%) is assumed. (Right) The cross sections of the production processes  $e^+e^- \rightarrow hZ$ ,  $e^+e^- \rightarrow H\nu_e\bar{\nu}_e$ ,  $e^+e^- \rightarrow He^+e^-$ ,  $e^+e^- \rightarrow t\bar{t}H$ ,  $e^+e^- \rightarrow HHZ$  and  $e^+e^- \rightarrow HH\nu_e\bar{\nu}_e$  as a function of the collision energy for the mass of 125 GeV. No polarization is assumed for the initial electron and positron beams.

Relative Higgs coupling measurements in % at various future colliders (when combined with HL-LHC results) based on on the kappa framework. Taken from the Snowmass 2021 Report of the Topical Group on Higgs Physics for the Energy Frontier.

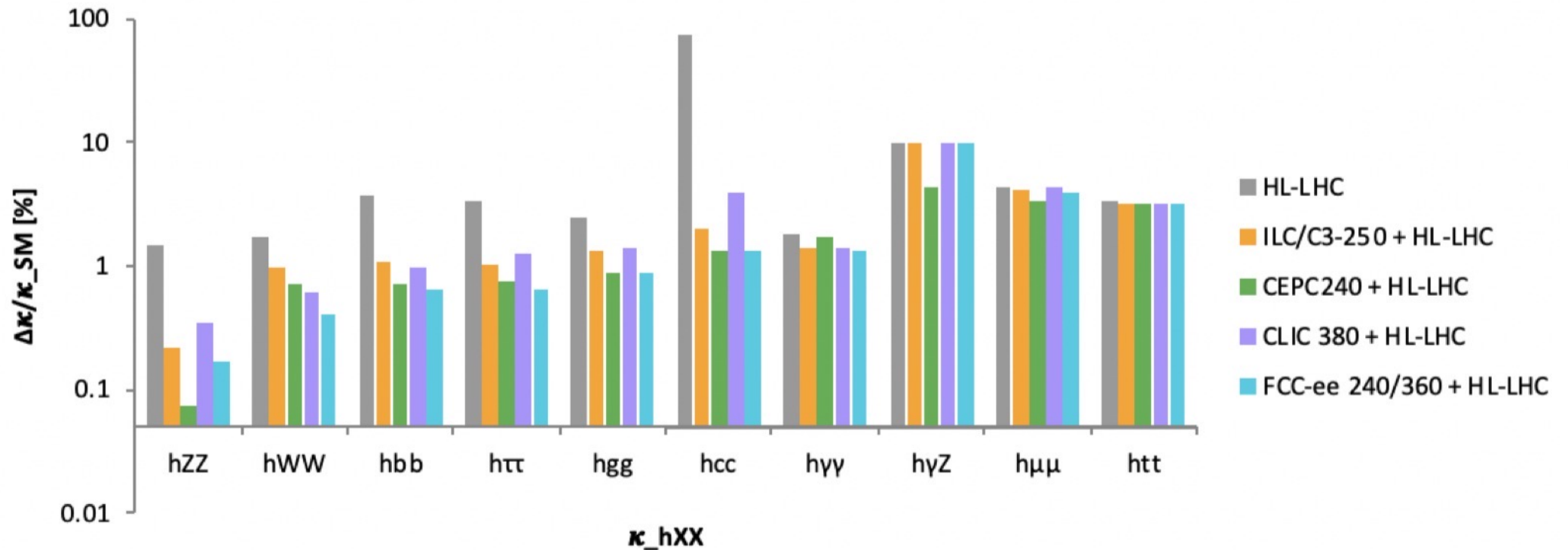
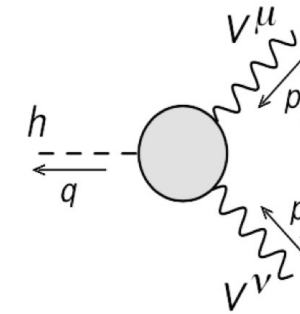


FIG. 19: Projected relative Higgs coupling measurements in % when combined with HL-LHC results. All values assume no beyond the Standard Model decay modes. In addition, only initial stages are shown for near-term colliders: This corresponds to  $3 ab^{-1}$  and two interaction points (IPs), ATLAS and CMS, for the HL-LHC at 14 TeV,  $2 ab^{-1}$  and 1 IP at 250 GeV for ILC/C<sup>3</sup>,  $20 ab^{-1}$  and 2 IP at 240 GeV for CEPC,  $1 ab^{-1}$  and 1 IP at 380 GeV for CLIC, and  $5 ab^{-1}$  and 4 IP at 240 GeV for FCC-ee. Note that the HL-LHC  $\kappa_{hcc}$  projection uses only the CMS detector and is an upper bound [60].

# Importance of higher dimensional operators



example:  $h Z Z$  vertex

$$T^{\mu\nu}(p_1, p_2) = F_1 g^{\mu\nu} + F_2(p_1 \cdot p_2 g^{\mu\nu} - p_1^\nu p_2^\mu) + F_3 \epsilon^{\mu\nu\alpha\beta} p_{1\alpha} p_{2\beta}$$

where the form factors  $F_1, F_2$  and  $F_3$  depend on Lorentz invariant combinations of the kinematic variables.

$F_1$  corresponds to the tree-level SM interaction,  $\mathcal{L}_{\text{int}} = h Z_\mu Z^\mu$

$F_2$  corresponds to the CP-even effective interaction,  $\mathcal{L}_{\text{eff}} = h F_{\mu\nu} F^{\mu\nu}$

$F_3$  corresponds to the CP-odd effective interaction,  $\mathcal{L}_{\text{eff}} = h F_{\mu\nu} \tilde{F}^{\mu\nu}$



**Caution:** Higher dimensional operators in SMEFT may not account for all BSM Higgs phenomena if additional relatively light scalars exist.

## Higgs boson coupling uncertainties based on a SMEFT analysis

The set of SMEFT operator coefficients is taken as a subset of the full set of dimension 6 operators in the Warsaw basis. The effective Lagrangian is given by  $\mathcal{L} = \mathcal{L}_{SM} + \mathcal{L}_6$  where

$$\mathcal{L}_6 = \mathcal{L}_H + \mathcal{L}_{W,B} + \mathcal{L}_{\Phi\ell} + \mathcal{L}_{\Phi q} + \mathcal{L}_{\Phi f} + \mathcal{L}_g .$$

The dimension 6 terms depending only on the Higgs and vector boson fields are:

$$\begin{aligned} \mathcal{L}_H &= \frac{c_H}{2v^2} (\partial_\mu \Phi^\dagger \Phi)^2 + \frac{c_T}{2v^2} \left( \Phi^\dagger \overleftrightarrow{D}^\mu \Phi \right) \left( \Phi^\dagger \overleftrightarrow{D}_\mu \Phi \right) - \frac{\lambda c_6}{v^2} (\Phi^\dagger \Phi)^3 \\ \mathcal{L}_{W,B} &= \frac{g^2 c_{WW}}{v^2} (\Phi^\dagger \Phi) W_{\mu\nu}^a W^{a\mu\nu} + \frac{2gg' c_{WB}}{v^2} (\Phi^\dagger t^a \Phi) W_{\mu\nu}^a B^{\mu\nu} \\ &\quad + \frac{g'^2 c_{BB}}{v^2} (\Phi^\dagger \Phi) B_{\mu\nu} B^{\mu\nu} + \frac{c_{3W}}{6v^2} \epsilon_{abc} W_\mu^{a\nu} W_\nu^{b\rho} W_\rho^{c\mu} \end{aligned}$$

Terms depending on the Higgs fields and the electron fields are:

$$\begin{aligned} \mathcal{L}_{\Phi\ell} = & \frac{c_{\Phi L}}{v^2} \left( \Phi^\dagger i \overleftrightarrow{D}_\mu \Phi \right) (\bar{L}^\dagger \gamma^\mu L) + \frac{4c'_{\Phi L}}{v^2} \left( \Phi^\dagger t^a i \overleftrightarrow{D}_\mu \Phi \right) (\bar{L}^\dagger t^a \gamma^\mu L) \\ & + \frac{c_{\Phi E}}{v^2} \left( \Phi^\dagger i \overleftrightarrow{D}_\mu \Phi \right) (\bar{e}^\dagger \gamma^\mu e) \end{aligned}$$

where  $L$  and  $e$  are the left- and right-handed fields of the first lepton generation and  $t^a = \sigma^a/2$  is the weak isospin generator. The dimension 6 term that shifts the Higgs- $\tau$  Yukawa coupling is

$$\mathcal{L}_{\Phi\tau} = \frac{y_\tau c_\tau}{v^2} (\Phi^\dagger \Phi) (\bar{L}_\tau \cdot \Phi e_\tau)$$

and the other operators that contribute to scalar couplings are constructed in a similar way. The operator

$$\mathcal{L}_g = \frac{g_s^2 c_{gg}}{v^2} (\Phi^\dagger \Phi) G_{\mu\nu}^a G^{a\mu\nu}$$

shifts the Higgs boson partial width to gluons.

coupling	2/ab-250	+4/ab-500	5/ab-250	+1.5/ab-350
	pol.	pol.	unpol.	unpol.
$hZZ$	0.50	0.35	0.41	0.34
$hWW$	0.50	0.35	0.42	0.35
$hb\bar{b}$	0.99	0.59	0.72	0.62
$h\tau\tau$	1.1	0.75	0.81	0.71
$hgg$	1.6	0.96	1.1	0.96
$hc\bar{c}$	1.8	1.2	1.2	1.1
$h\gamma\gamma$	1.1	1.0	1.0	1.0
$h\gamma Z$	9.1	6.6	9.5	8.1
$h\mu\mu$	4.0	3.8	3.8	3.7
$htt$	-	6.3	-	-
$hhh$	-	20	-	-
$\Gamma_{tot}$	2.3	1.6	1.6	1.4
$\Gamma_{inv}$	0.36	0.32	0.34	0.30
$\Gamma_{other}$	1.6	1.2	1.1	0.94

TABLE VII: Projected uncertainties in the Higgs boson couplings computed within the SMEFT framework and including projected improvements in precision electroweak measurements, as described in the ILC reports and the FCC-ee CDR [51, 70, 71].



As noted in the Snowmass 2021 Report of the Topical Group on Higgs Physics for the Energy Frontier:

“Despite their different strategies, all  $e^+e^-$  Higgs factory proposals lead to very similar projected uncertainties on the Higgs boson couplings. The higher luminosity proposed for circular  $e^+e^-$  machines is compensated by the advantages of polarization at linear colliders, yielding very similar projected sensitivity for the precision of Higgs couplings. In combination with the measurement of the rate of Zh events with an  $h \rightarrow ZZ$  decay, a model-independent determination of the Higgs total width can be obtained at an  $e^+e^-$  collider. The analysis of the other Higgs decays similarly provides a set of model-independent Higgs partial width and coupling measurements.”

Remark: regarding the last point above, a precision measurement of the Higgs mass is needed to compare the experimentally measured  $e^+e^- \rightarrow Zh$  cross section with the theoretical prediction.

Taken from “The International Linear Collider: Report to Snowmass 2021”

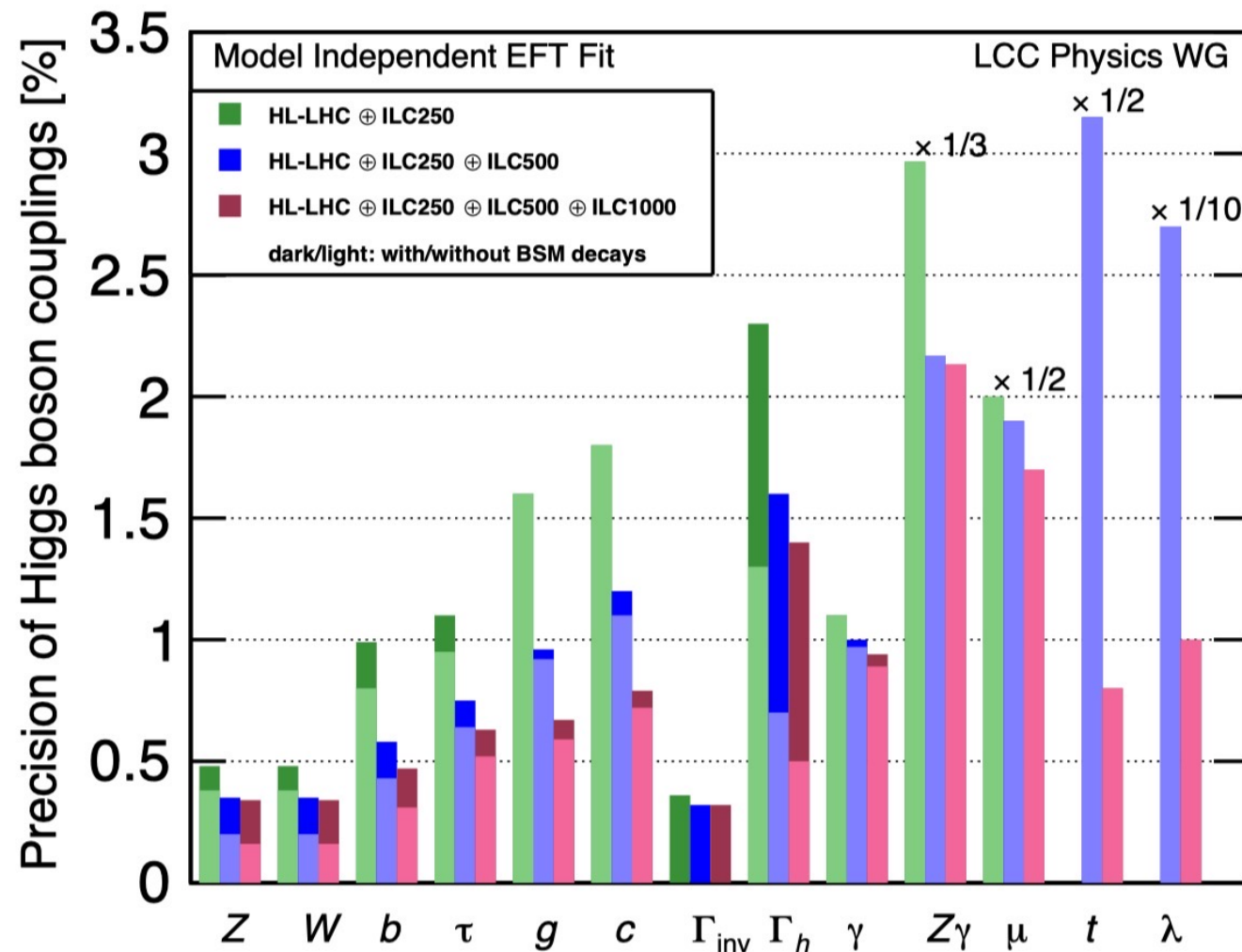
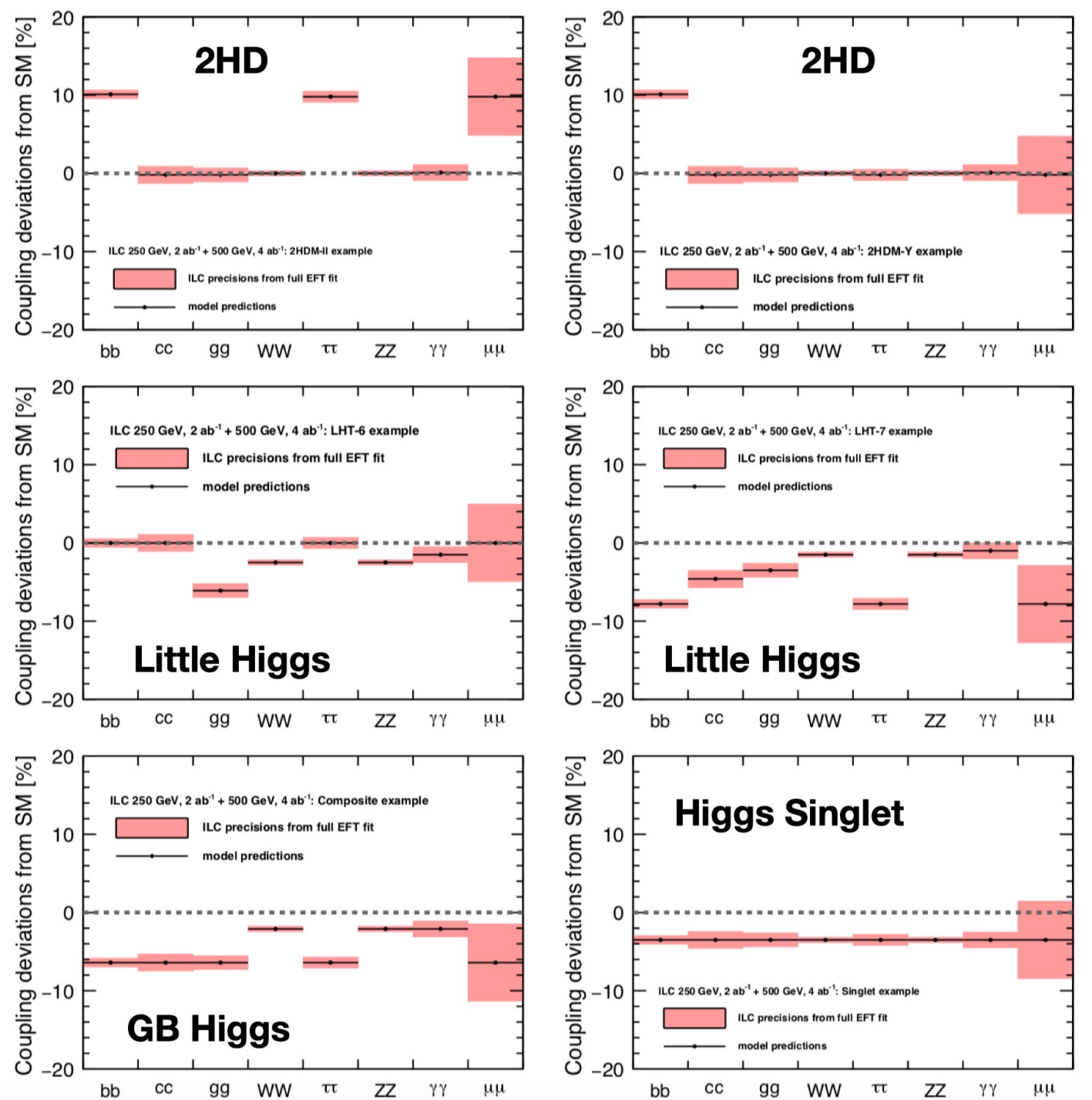


Figure 12.1: Projected Higgs boson coupling uncertainties for ILC250, ILC500, and ILC1000, also incorporating results expected from the HL-LHC, based on the SMEFT analysis described in the text. The darker bars show the results allowing invisible and exotic Higgs decay channels; the lighter bars assume that these BSM decays are not present. The column  $\lambda$  refers to the  $HHH$  coupling. In the last four columns, all bars are rescaled by the indicated factor. From [428].

A number of specific models with large Higgs coupling deviations due to new particles that are out of reach at the HL-LHC were collected in T. Barklow et al., arXiv:[1708.08912](https://arxiv.org/abs/1708.08912).

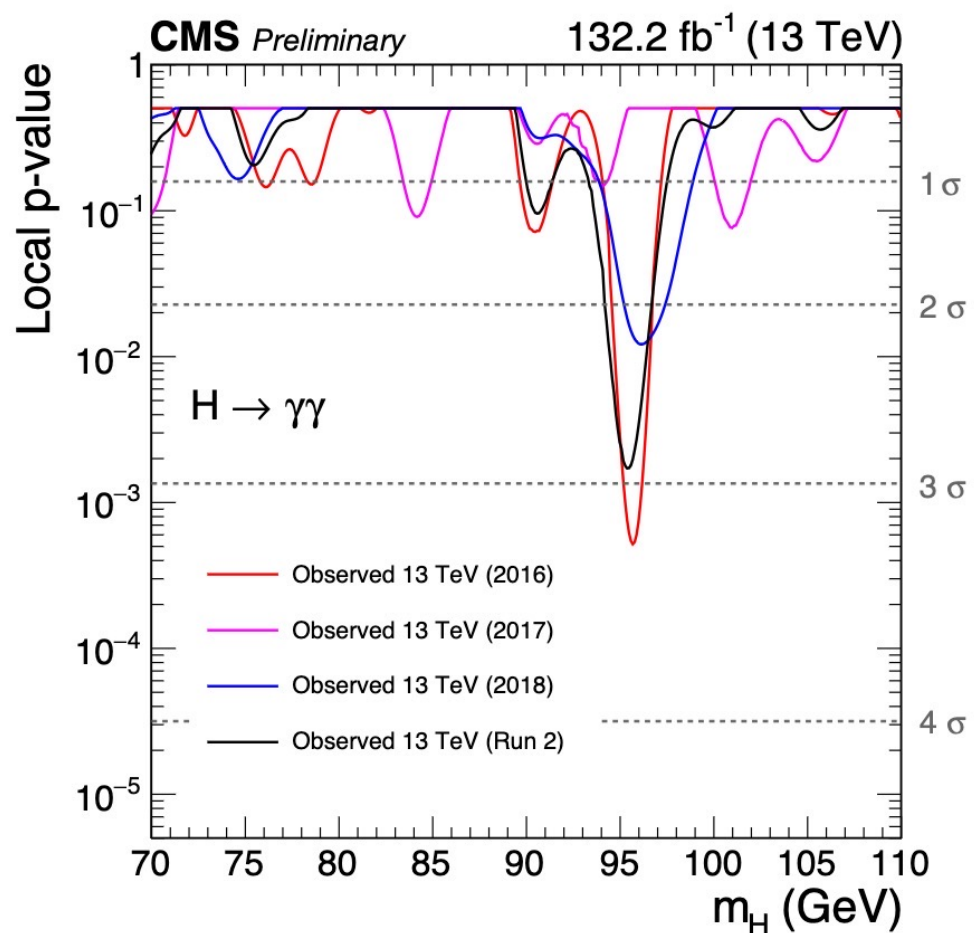
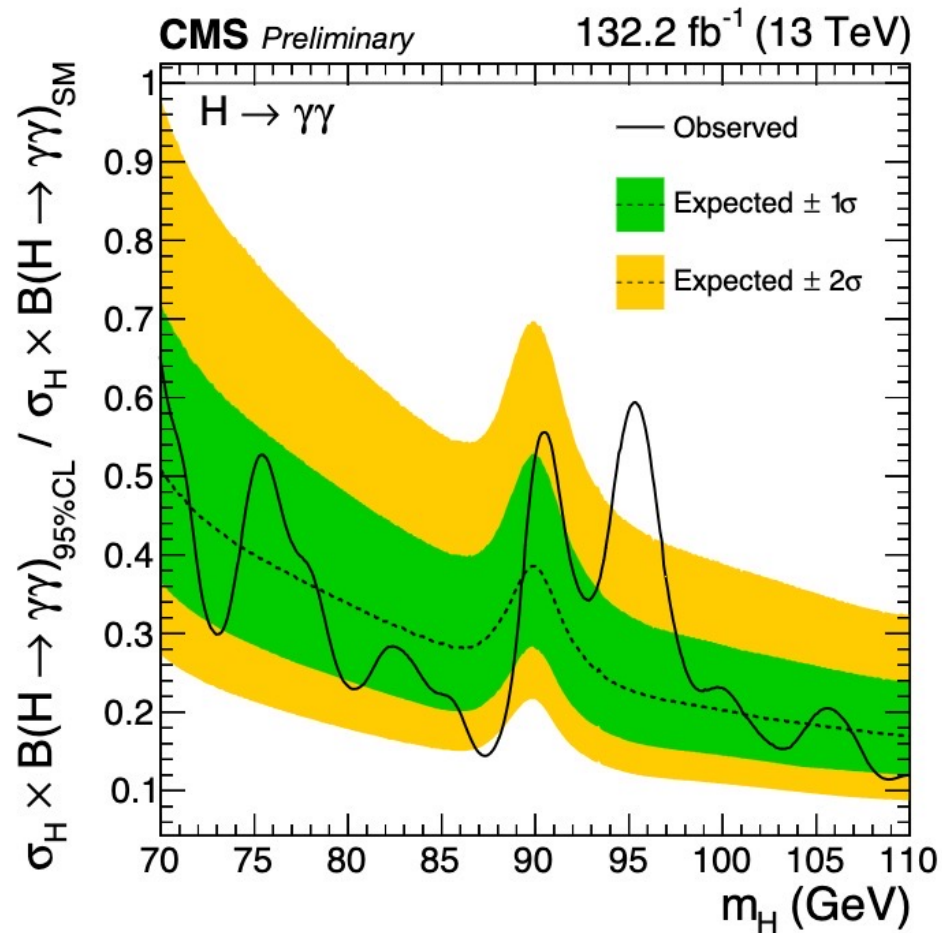
Visualization of the deviations of Higgs couplings from the SM for the new physics discussed in arXiv:[1708.08912](https://arxiv.org/abs/1708.08912), compared to the uncertainties in the measurements expected from a fit to ILC data at 250 and 500 GeV.



# What if additional light states are present?

- Higgs boson decays into dark sector particles
- Higgs boson decays into new light states
  - $h \rightarrow aa$  (e.g. N2HDM, NMSSM, etc.)
  - $h \rightarrow \gamma \gamma_d$  ( $\gamma_d =$  dark photon)
- Other new scalars [H(95)?]

Invisible Higgs decays are accessible at a Higgs factory via  $e^+e^- \rightarrow Zh$  production, where the recoiling Z tags the Higgs events.



Taken from CMS PAS HIG-20-002

Figure 7: The observed local  $p$ -values for an additional SM-like Higgs boson as a function of  $m_H$ , from the analysis of the data from 2016, 2017, 2018, and their combination.

# Importance of the Triple Higgs (hhh) coupling

In the Standard Model, the dynamics of EWSB is governed by the Higgs scalar potential. However, we have very limited experimental information on the shape of this potential away from its minimum.

The hhh coupling provides critical information on the nature of the electroweak phase transition.

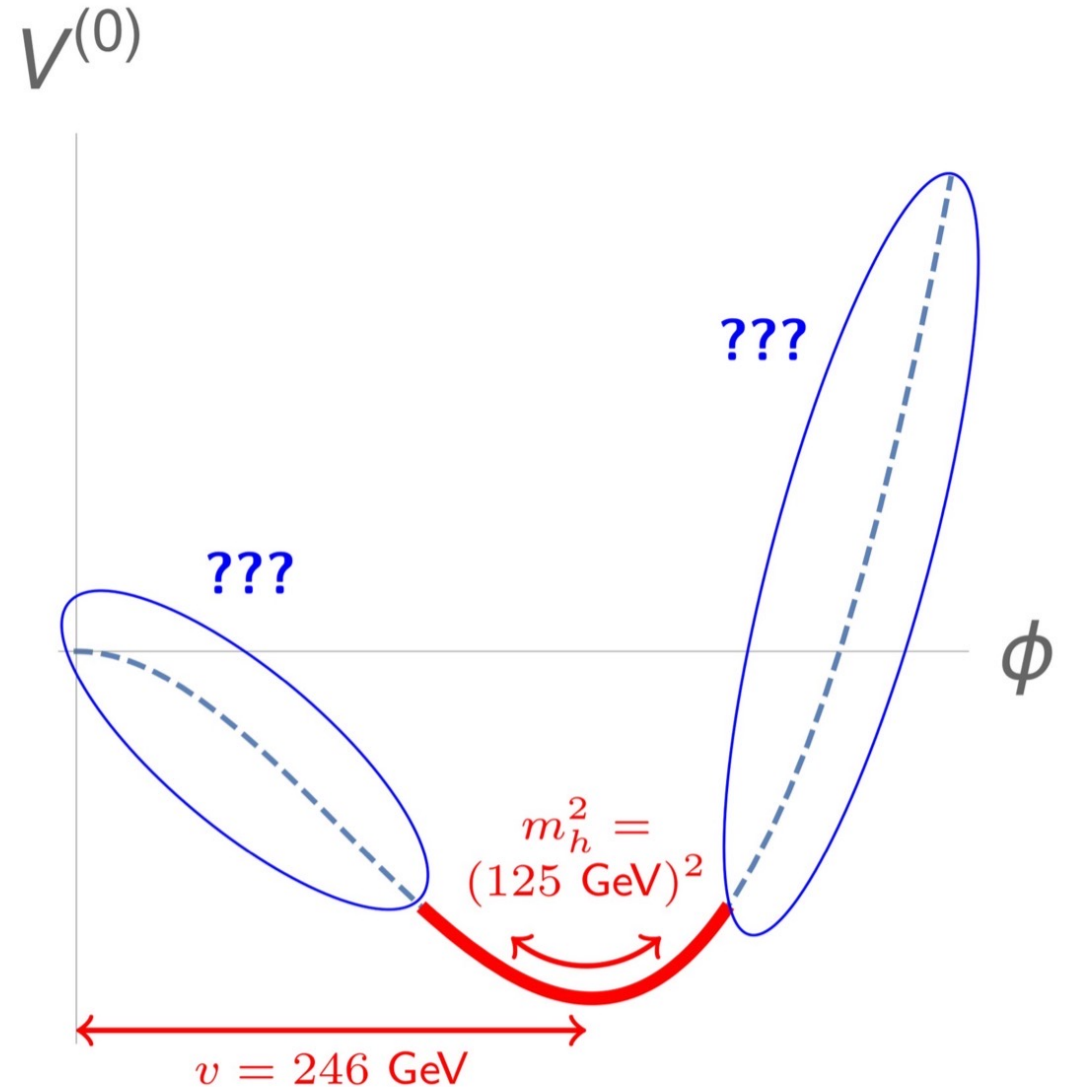


Figure courtesy of Johannes Braathen

# Key ingredients for electroweak baryogenesis

- Strong first order electroweak phase transition
- New sources of CP-violation (consistent with limits on the edm of the electron)

Requires new BSM physics that generates an enhancement of the hhh coupling (denoted by  $\kappa_\lambda$ ). Examples include extended Higgs sectors which can induce large radiative corrections to hhh coupling in certain parameter regimes.

Added benefit: a strong electroweak phase transition can yield a detectable gravitational wave signal (in future experiments such as LISA).

# Measuring the hhh coupling via DiHiggs and Zh production

## ➤ DiHiggs production

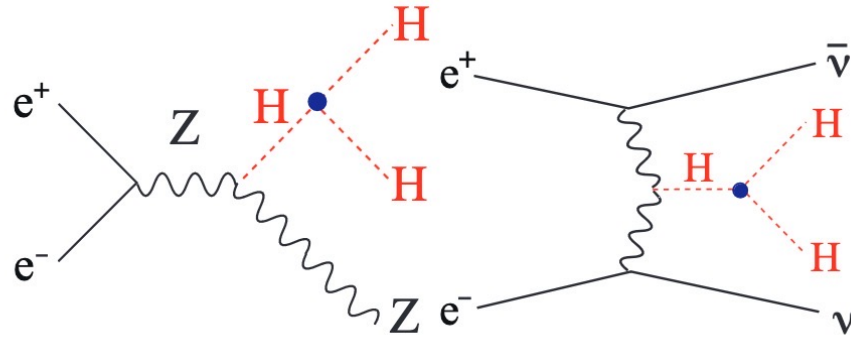


Figure 1.5. Typical diagrams for double Higgs boson production via off-shell Higgsstrahlung (Left) and  $W$ -boson fusion (Right) processes.

## ➤ One-loop correction to $Z^* \rightarrow Zh$ production

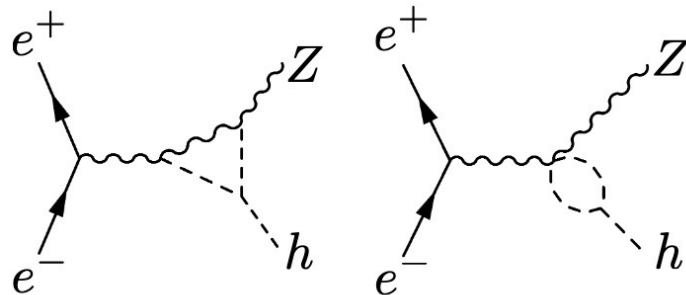


FIG. 1: NLO vertex corrections to the associated production cross section which depend on the Higgs self-coupling. These terms lead to a linear dependence on modifications of the self-coupling  $\delta_h$ .

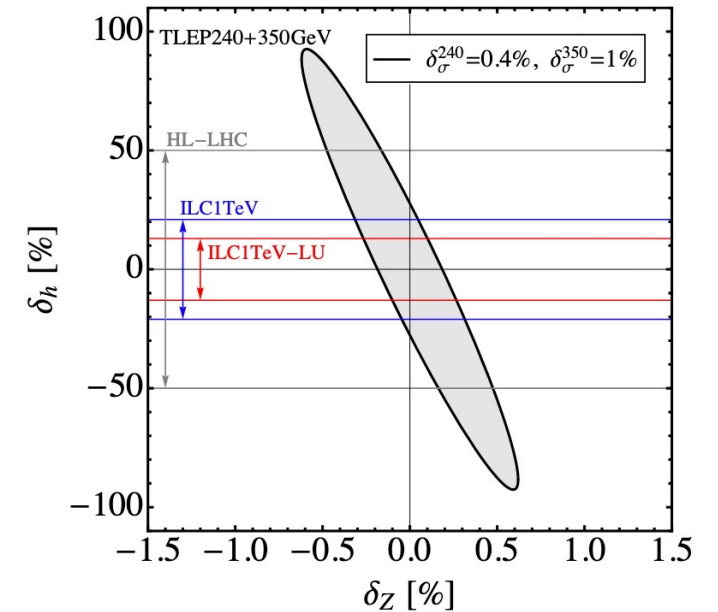
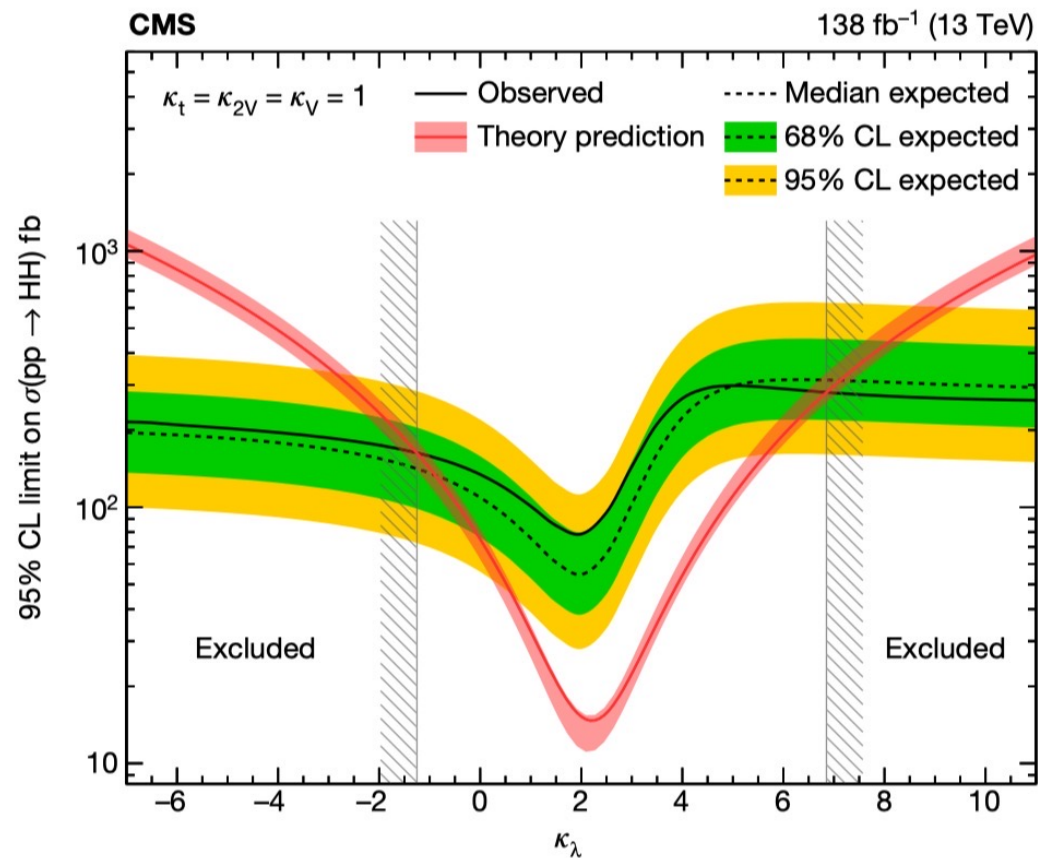
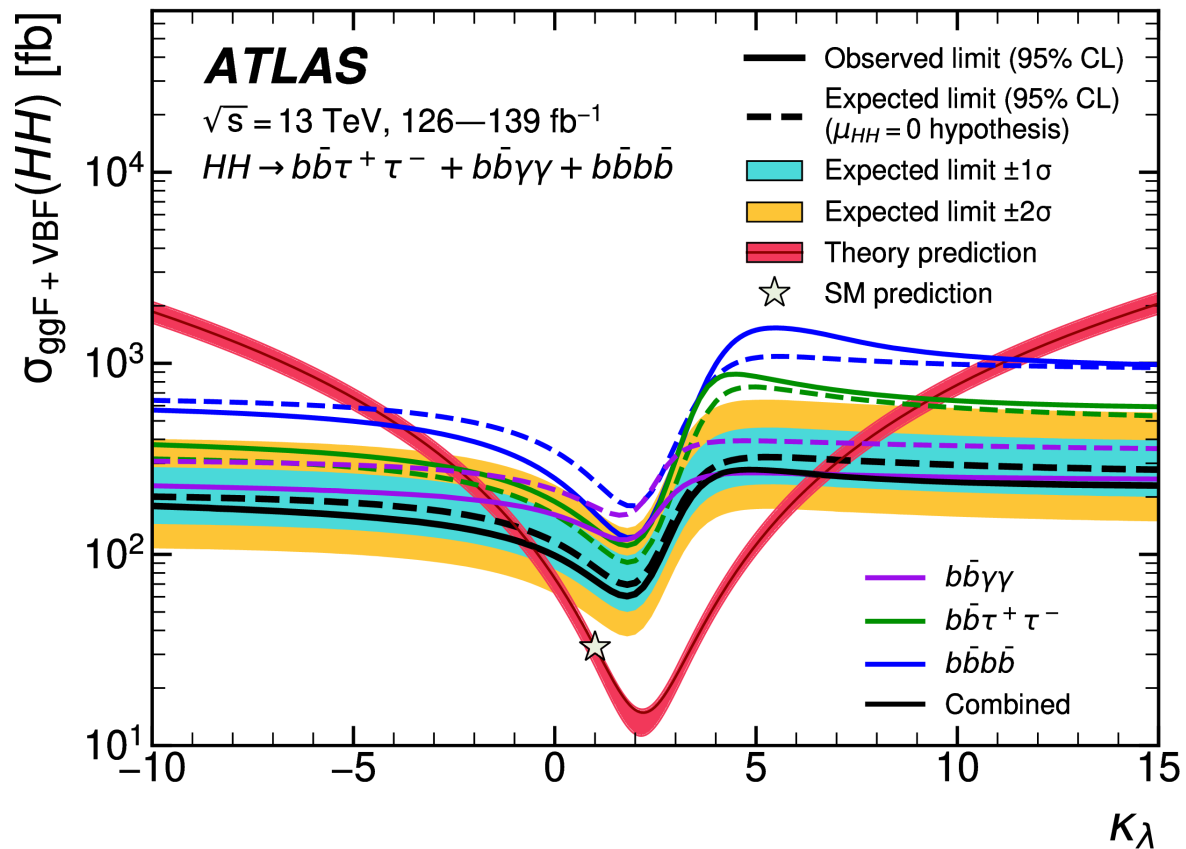
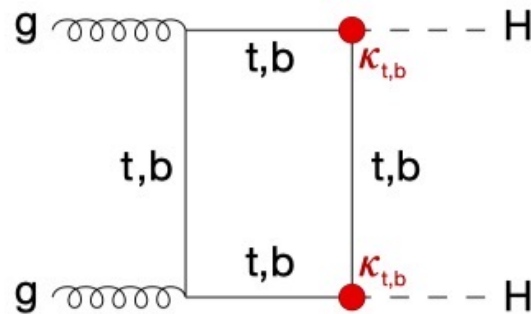
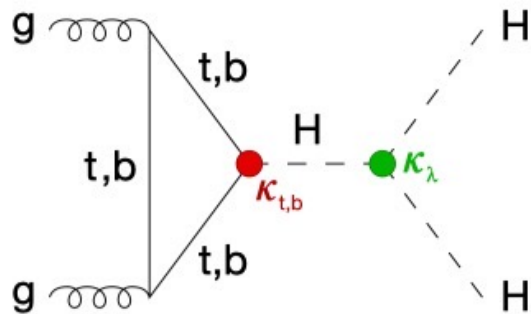


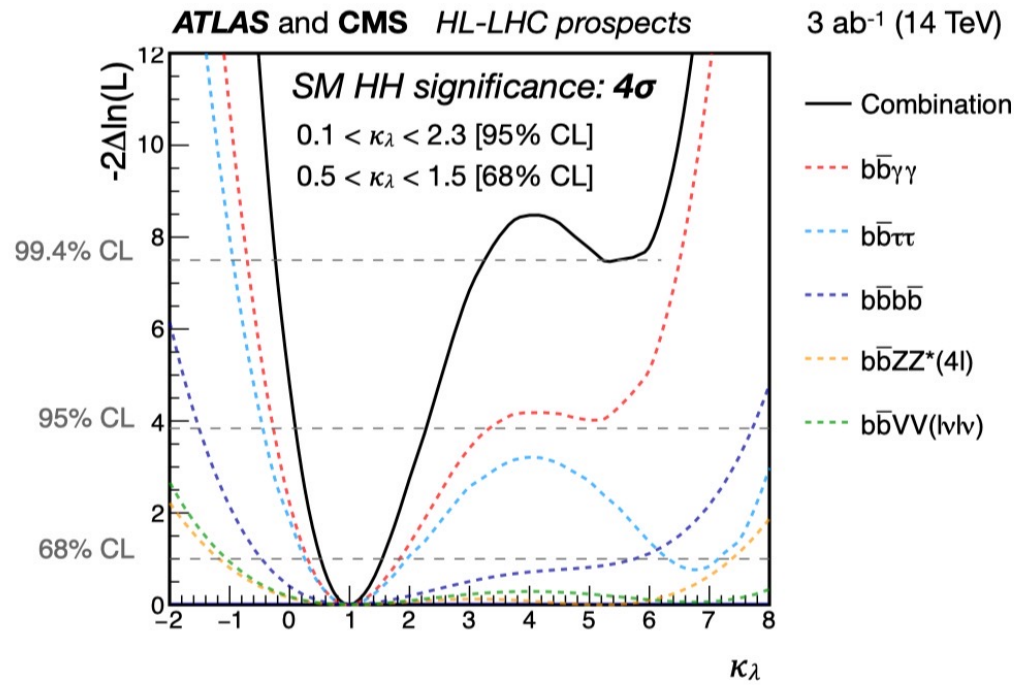
FIG. 3: Indirect  $1\sigma$  constraints possible in  $\delta_Z - \delta_h$  parameter space by combining associated production cross section measurements of 0.4% (1%-estimated) precision at  $\sqrt{s} = 240$  GeV, (350 GeV) in solid black. For large values of  $|\delta_h|$  this ellipse can only be considered qualitatively as the calculation is only valid to lowest order in  $\delta_h$ . The different scales should be noted. Direct constraints possible at the high luminosity LHC and 1 TeV ILC (with LU denoting luminosity upgrade)

Taken from Matthew McCullough, arXiv:1312.3322

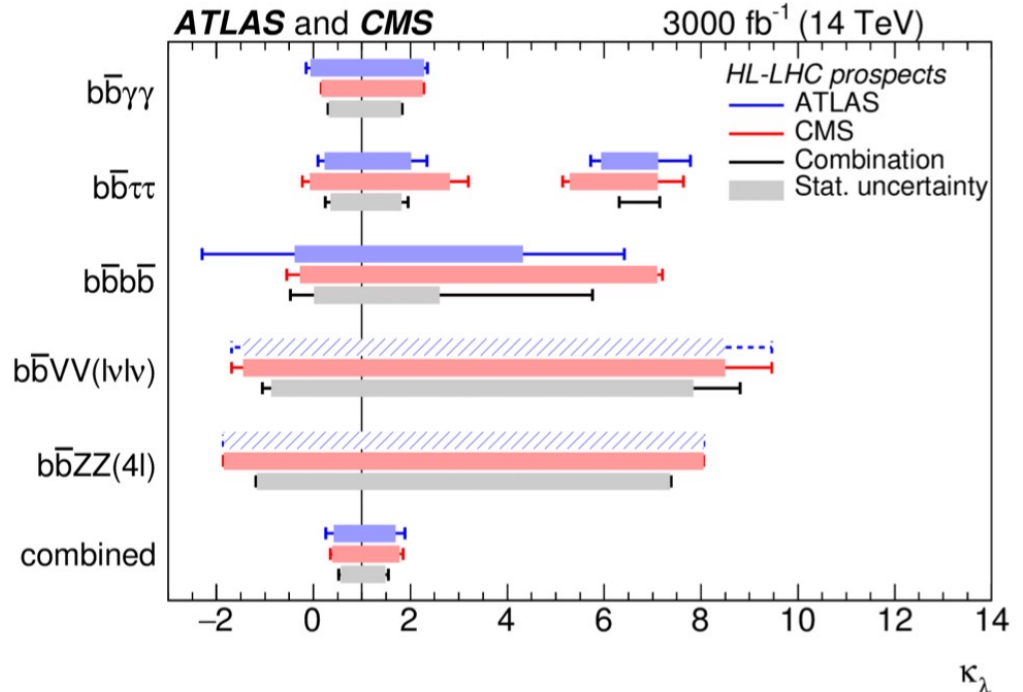


# What information can the LHC provide on $\kappa_\lambda$ ?





(a)

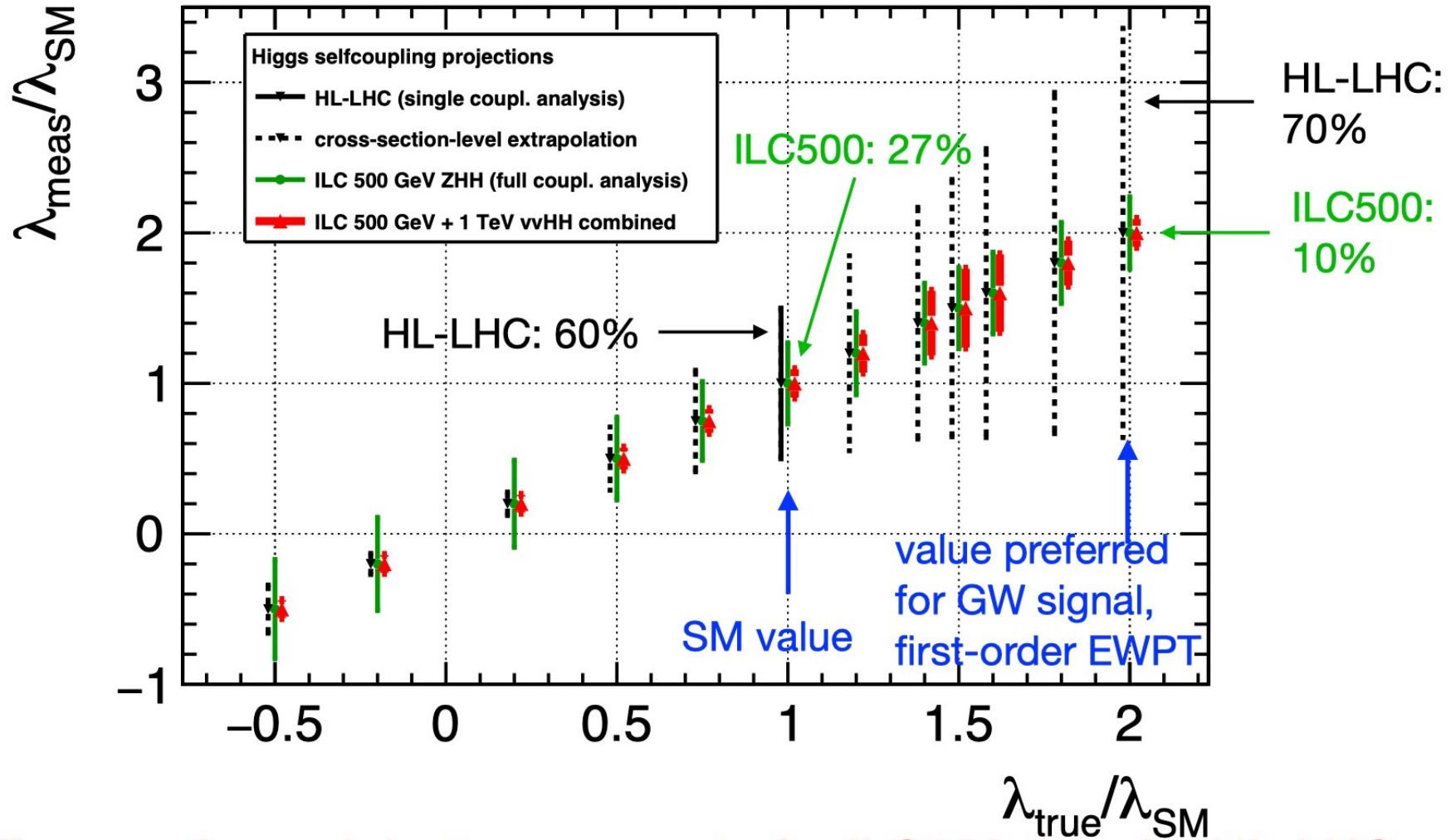


(b)

Fig. 66: (a) Minimum negative-log-likelihood as a function of  $\kappa_\lambda$ , calculated by performing a conditional signal+background fit to the background and SM signal. The coloured dashed lines correspond to the combined ATLAS and CMS results by channel, and the black line to their combination. The likelihoods for the  $HH \rightarrow b\bar{b}VV(l\nu l\nu)$  and  $HH \rightarrow b\bar{b}ZZ(4l)$  channels are scaled to  $6000 \text{fb}^{-1}$ . (b) Expected measured values of  $\kappa_\lambda$  for the different channels for the ATLAS in blue and the CMS experiment in red, as well as the combined measurement. The lines with error bars show the total uncertainty on each measurement while the boxes correspond to the statistical uncertainties. In the cases where the extrapolation is performed only by one experiment, same performances are assumed for the other experiment and this is indicated by a hatched bar.

# Prospects for measuring the trilinear Higgs coupling: HL-LHC vs. ILC

[J. List et al. '21]

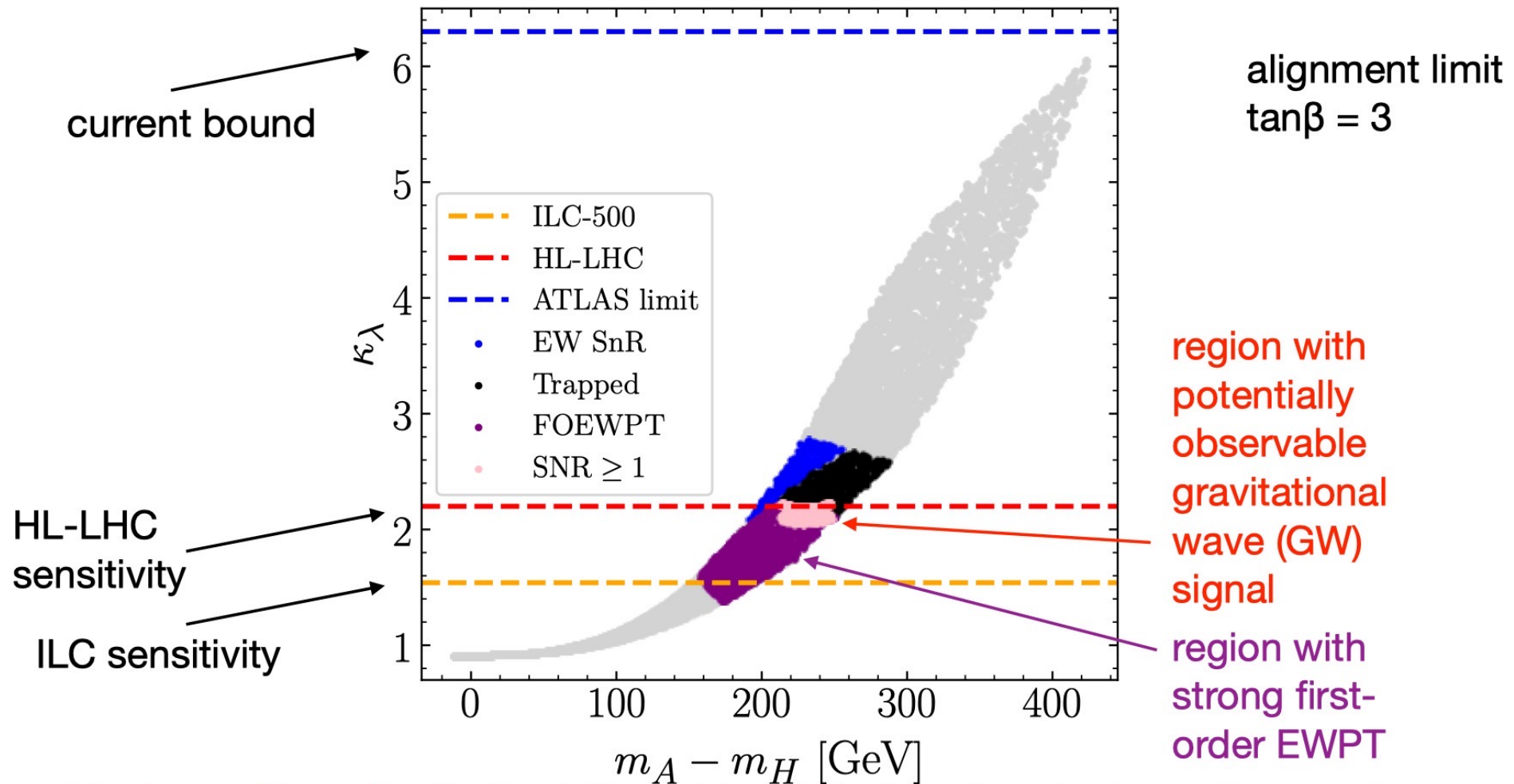


⇒ For  $\kappa_\lambda \approx 2$ : much better prospects for ILC500 than for HL-LHC

Reason: different interference contributions

# 2HDM, 1-loop predictions for the trilinear Higgs coupling vs. current bound and future sensitivities

[T. Biekötter, S. Heinemeyer, J. M. No, M. O. Olea, G. W. '2



⇒ Region with potentially detectable GW signal and strong first-order EWPT is correlated with significant deviation of  $\kappa_\lambda$  from SM value

Taken from  
Physics Briefing  
Book (Input for  
the European  
Strategy for  
Particle Physics  
Update 2020),  
arXiv:[1910.11775](https://arxiv.org/abs/1910.11775)

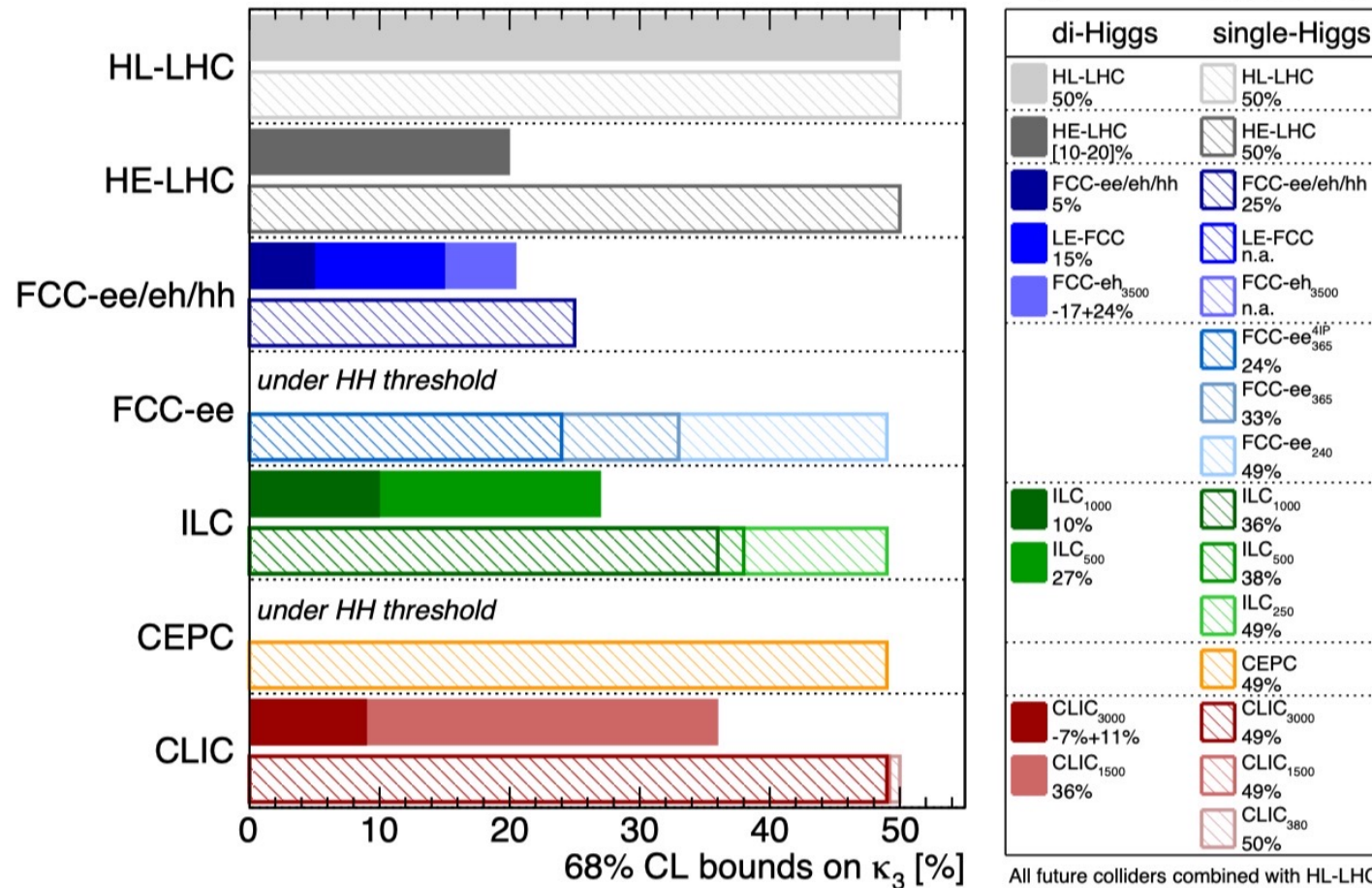


Fig. 3.10: Sensitivity at 68% probability on the Higgs self-coupling parameter  $\kappa_3$  at the various future colliders. All the numbers reported correspond to a simplified combination of the considered collider with HL-LHC, which is approximated by a 50% constraint on  $\kappa_3$ . For each future collider, the result from the single- $H$  from a global fit, and double- $H$  are shown separately. For FCC-ee and CEPC, double- $H$  production is not available due to the too low  $\sqrt{s}$  value. FCC-ee is also shown with 4 experiments (IPs) as discussed in Ref. [75] although this option is not part of the baseline proposal. LE-FCC corresponds to a  $pp$  collider at  $\sqrt{s} = 37.5$  TeV.

# Parting Messages

- “The case for an  $e^+e^-$  Higgs factory is strong today, but it can be made stronger with concerted effort, especially in the relation between models and their impact on the Higgs properties.” (Michael Peskin)
- Precision Higgs measurements at an  $e^+e^-$  Higgs factory can potentially yield deviations from the SM that indicate the existence of new, undiscovered particles at the TeV scale that lie beyond the reach of HL-LHC.
- Higgs factories also provide sensitive probes of new feebly-interacting particles via the Higgs portal.
- At  $e^+e^-$  Higgs factories with CM energies of 500 GeV and above, access to the triple-Higgs coupling and probes of new (scalar-mediated) sources of CP violation can address the nature of the electroweak phase transition.